Infrared Physics & Technology 55 (2012) 431–441

Contents lists available at SciVerse ScienceDirect

Infrared Physics & Technology

journal homepage: www.elsevier.com/locate/infrared

Jamming effect analysis of infrared reticle seeker for directed infrared countermeasures

Tae-Wuk Bae [a,*], Byoung-Ik Kim [b], Young-Choon Kim [c], Sang-Ho Ahn [d]

[a] Stanford Center for Image Systems Engineering, Stanford University, CA 94305, USA
[b] School of Electrical Engineering and Computer Science, Kyungpook National University, South Korea
[c] Dept. of Information and Communication Engineering, Youngdong University, South Korea
[d] Dept. of Electronic Engineering, Inje University, South Korea

HIGHLIGHTS

- The purpose of jamming toward missiles is making missiles miss the target.
- We implemented a reticle seeker simulation tool for jamming effect analysis.
- Jamming effect depends on frequency, phase and intensity of jammer signal.
- For maximum jamming effect, jammer frequency and reticle frequency must be same.
- We evaluated jamming effect by using jamming correlation coefficient.

ARTICLE INFO

Article history:
Received 16 January 2012
Available online 26 May 2012

Keywords:
Spin-scan reticle seeker
Con-scan reticle seeker
Infrared
DIRCM
Jamming effect

ABSTRACT

In directed infrared countermeasures (DIRCM), the purpose of jamming toward missiles is making missiles miss the target (aircraft of our forces) in the field of view. Since the DIRCM system directly emits the pulsing flashes of infrared (IR) energy to missiles, it is more effective than present flare method emitting IR source to omni-direction. In this paper, we implemented a reticle seeker simulation tool using MATLAB-SIMULINK, in order to analyze jamming effect of spin-scan and con-scan reticle missile seeker used widely in the world, though it was developed early. Because the jammer signal has influence on the missile guidance system using its variable frequency, it is very important technique among military defense systems protecting our forces from missiles of enemy. Simulation results show that jamming effect is greatly influenced according to frequency, phase and intensity of jammer signal. Especially, jammer frequency has the largest influence on jamming effect. Through our reticle seeker simulation tool, we can confirm that jamming effect toward missiles is significantly increased when jammer frequency is similar to reticle frequency. Finally, we evaluated jamming effect according to jammer frequencies, by using correlation coefficient as an evaluation criterion of jamming performance in two reticle missile seekers.

1. Introduction

As infrared (IR) guided missile has been developed, various IR small target detection methods such as spatial filter based method [1–5], morphology based method [6,7], temporal based method [8–10], have been researched in order to detect missile early. To cope with the detected IR guided missile actively, various infrared countermeasures (IRCM) also have been developed simultaneously [11]. The IRCM is essential in modern war in order to protect targets such as aircrafts or ground vehicles from advanced missiles that could be a threat and damage to those. In general, IR missiles utilize a thermal energy radiated or reflected by targets. In the war area for 20 years, about 90% of airplanes were damaged by the IR guided missile. So, the IRCM is actively being developed to protect aircrafts against an attack of IR missiles [12]. IRCM is divided into flare method and jammer method. The flare method emits jamming signal of high radiation energy which includes IR band of protective objects such as aircraft, and vehicle. The flare method is vulnerable to approach attacks and limited in its amount of loading and continuative launch. And recent developed missiles have, moreover, some techniques discriminating targets and flare. The jammer method is also divided into omni-directional jammer method and directed jammer method [13]. The omni-directional jammer method uses higher luminance light with electrical filaments or a fuel burner as jamming source. Since this method emits IR source to omni-direction, it is a lot of power consumption and does not inject strong jamming signal to missile seeker. In order

* Corresponding author.
E-mail address: nanninggo@gmail.com (T.-W. Bae).

1350-4495/$ - see front matter © 2012 Elsevier B.V. All rights reserved.
http://dx.doi.org/10.1016/j.infrared.2012.05.001

to solve this weak-point, directed infrared countermeasures (DIRCM), the directed jammer method have been developed [14]. Because the directed jammer method uses higher luminance lamps or laser for concentrating on jamming energy into missile seeker, it is not consuming and can emit jamming source continuatively. And it can counteract scanning methods of various missile seekers. Because DIRCM are more effective than the present flare method or the omni-directional jammer method using higher luminance lamp, so its development and research are progressing in these days. Due to these reasons, this paper analyzes the jamming effect of the DIRCM in current used reticle seekers.

Usually IR missiles have a single IR detector, and reticle with a form of saw-tooth on a circle plane used to make a signal for detecting targets. But, recently, a quadrant-detector using four detectors and an imaging seeker using the focal plane array (FPA) detector were developed. The reticle seeker with a single detector is classified as three type of scanning method: spin-scan, con-scan, and rosette-scan. Until now, many researchers have researched for various reticle seekers [15–18]. However, these researches were about a reticle type and its signal processing in a viewpoint of missile. In imaging viewpoint, a jammer signal irradiating toward an upcoming missile is greatly depends on the type of seeker. Therefore, the jamming effect analysis of reticle seeker is required for development of more effective jammer signal.

This paper implemented a reticle seeker simulator using MATLAB-SIMULINK in order to analyze jamming effect of spin-scan and con-scan reticle seeker used widely in the world, though it was developed early. The implemented simulator includes a tracking process of target in field of view (FOV) of seeker and a guidance loop for an approach of a missile. We analyze jamming effect by examining target position according to changes of frequency and intensity of jammer signal. Simulation results show that jamming effect is significantly increased when jammer frequency is similar to reticle frequency, through a 3D trajectory of missile motion by jamming.

The organization of this paper is as follows. Section 2 explains the atmospheric transmission of IR band as basic knowledge of IR. In Section 3, an IR guided missile with reticle seeker is introduced. In Section 4, the DIRCM jamming is provided based on signal processing of the reticle seeker. Section 5 explains the reticle seeker simulator implemented by MATLAB-SIMULINK, and then jamming effect analysis is performed and conclusions are given in Section 6.

2. Atmospheric transmission of IR band

Electro-optical sensors (IR sensor) used in an advanced weapon systems uses the wavelength of visible light and IR bands. Generally, the electromagnetic spectrum is divided into ultraviolet band (0.1–0.38 μm), visible band (0.38–0.76 μm), IR band (0.76–12 μm), and Radio/Micro-wave band (12 μm–) according to its wavelength. Especially, the IR band is divided into near-wavelength IR (NWIR, 0.77–3 μm), NWIR), middle-wavelength IR (MWIR, 3–6 μm), and long-wavelength IR (LWIR, 6–15 μm), and extreme-wavelength IR (EWIR, 15 μm–1 mm). Like electromagnetic waves, the IR band has optical properties such as reflection, refraction, and diffraction between visible band and Radio/Microwave band, and is propagated at the speed of light. And the IR band is optically focused and diffused through lens and prism, etc. and passes through opaque objects unlike visible light. But the radiation energy of the IR is absorbed by vapor ingredients such as atmospheric scattering, gas molecules, aerosols, rain, snow, fog, haze, and smog. So, its atmospheric transmission characteristic is attenuated according to its wavelength. Among IR band, EWIR band has little ability to permeate the atmosphere. However, MWIR and LWIR band has superior transmission characteristics compared to the other IR band. So, these bands with good transmission are applied to sensors and optics in IR imaging system.

Fig. 1 shows atmospheric transmissions of IR band for a test case through PcMODTRAN5, an atmospheric analysis tool. The PcMODTRAN5, which is co-developed by the US Air Force Research Laboratory and Ontar Corp., calculates the spectral transmittance and radiance for arbitrary atmospheric paths from the microwave through the visible bands [19]. The basic atmospheric calculation in PcModWin5 uses the MODTRAN5 model. MODTRAN5 performs accurate and speedy calculations from the UV through the visible, infrared and microwave spectrum (0–50,000 cm^{-1}). Calculations in the visible and ultraviolet spectral regions (>22,600 cm^{-1}) are performed at lower spectral resolution (20 cm^{-1}), while those in the IR and longer wavelengths are done at 0.1 cm^{-1} resolution. Fig. 1a shows a path (Zenith angle: 45 degree) from an observer looking up at the sky, at 1.5 km altitude. This case uses the 1976 US Standard atmospheric model and slant path geometry with the rural aerosol model and visibility of 23 km. Fig. 1b shows the atmospheric transmittance in the 0–15 μm spectral region. The blue dotted line and green[1] dashed line represent the transmittance of H_2O and Ozone, and the red solid line appears total transmittance. We can show that MWIR and LWIR band have superior transmission characteristics, compared to NWIR and EWIR bands. So, these bands are important bands for the military application using the IR sensor in IR imaging system.

3. IR guided missile with reticle seeker

In general, IR missiles utilize thermal energy radiated or reflected by targets. Fig. 2 shows an optical structure of a heat-seeking missile seeker containing a primary mirror and secondary mirror. Through two mirrors and a reticle, radiant energy from targets is focused to an IR detector [20]. And then, target signal passing the IR detector goes through a signal processing block and a target tracking block to detect the azimuth angle of targets, as shown in Fig. 3. As known in the name of reticles, a spin-scan reticle has rotating (spinning) reticle on a fixed optics and a con-scan reticle has a reflection mirror spinning with cone type in front of a fixed reticle [14].

As shown in Fig. 3, block diagram of a typical IR guided missile contains a basic tracking and a missile guidance loop [14]. The missile's driving inputs stem from target's motions and radiations seen through the atmosphere, at the seeker. And it can contain jamming radiation. In the spin-scan reticle seeker, a target may be imaged on a spinning reticle. On the other hand, a target image is rotated on a stationary reticle in the con-scan reticle seeker. The modulated target radiation is sensed by an IR detector that converts that into an electrical signal. The sensed target radiation signal is converted to proper signal driving the seeker in order to close the tracking loop. And then, it is further demodulated to generate a necessary missile's turning rates for navigation and autopilot.

The tracking loop is simplified as a DC motor with the first-order transfer function [21]. And we used the proportional navigation guidance (PNG) to guide missiles for intercepting targets. The autopilot is modeled by a simple first-order lag system and its output is the fin commands that control missile motions [22]. In the PNG, missiles leads targets by flying to an interceptive point projected in front of targets. This provides the missile trajectory with the shortest flight path to the interceptive point in the engagement end game. To achieve an interception using PNG, the missile must have a range closure and control the LOS (line of

[1] For interpretation of color in Figs. 1, 4, 6, 12, 13, 15–17, 20, 21 the reader is referred to the web version of this article.

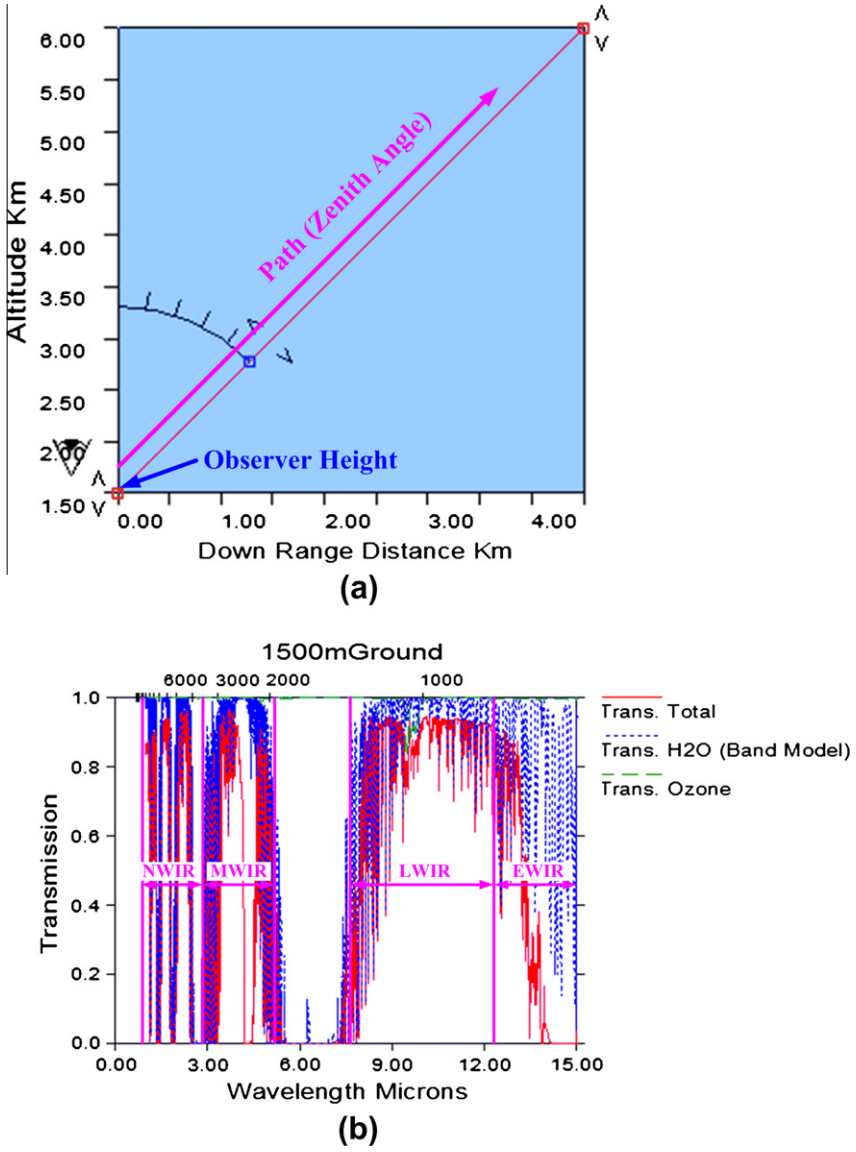

Fig. 1. Atmospheric transmission of IR band. (a) Path from observer and (b) its atmospheric transmittance.

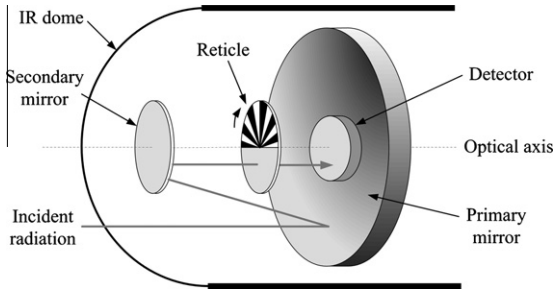

Fig. 2. Optical structure of heat-seeking missile seeker.

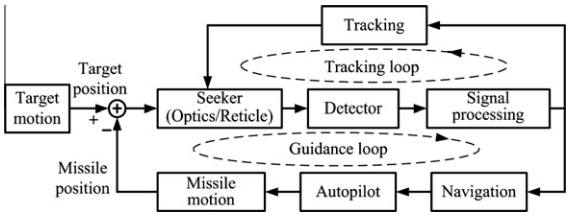

Fig. 3. Block diagram of typical IR guided missile.

sight) rotation rate ($\bar{\lambda}$). A simplified relation for the PNG can be stated as

$$a_n = NV_c\bar{\lambda} \tag{1}$$

where a_n, N, and V_c are the acceleration command, the navigation ratio (usually in the range of 3–5), and the closing velocity, respectively [23]. We implement the PNG in missile motion block of simulator shown in Fig. 3.

3.1. Spin-scan reticle seeker and its signal processing

The structure and the detector's output pulse of the spin-scan reticle seeker are shown in Fig. 4 [24,25]. The reticle has 12 initial spokes, 6 white (transparent) and 6 black (opaque) spokes. The white spokes pass the IR radiation of targets. On the contrary, the black spokes cut off that. And the lower gray part, the phasing sector, is semitransparent (passing 50% of the radiation). Fig. 4a shows the structure of the spin-scan reticle seeker. As IR targets

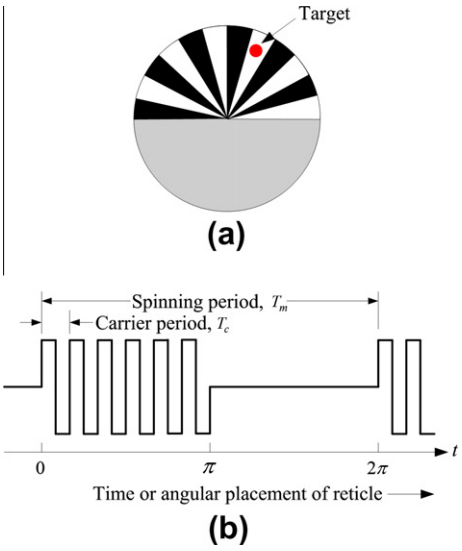

Fig. 4. (a) Structure and (b) its output pulse of spin-scan reticle seeker.

exist on transparent and opaque spokes, it generates the modulation signal as shown in Fig. 4b. The spinning frequency of the reticle seeker uses 100 Hz.

The signal processing procedure of the spin-scan reticle seeker is shown in Fig. 5. The carrier band-pass filter (BPF) extracts the carrier frequency. The amplitude modulation (AM) demodulator is used to detect the amplitude of the carrier pulse group and the envelope detector is mainly used for detecting its envelope. If targets move on the center of the reticle, the amplitude of the output pulse becomes smaller. If targets move on the outside from the center of the reticle, the amplitude of the output pulse becomes larger. This is similar to AM. So the AM demodulator can estimate the radial position and the phase detector estimates the azimuth angle of targets by comparing with the standard phase of the reticle.

3.2. Con-scan reticle seeker and its signal processing

Unlike the spin-scan reticle seeker, the reticle of a cons-can seeker is stationary and the target image is rotated on the reticle by a canted mirror that spins with a gyro (rotating magnet) [24,25]. Fig. 6a shows a spinning of a target on the con-scan reticle and its modulation signal is shown in Fig. 6b. The con-scan reticle uses the circular disk with a saw-tooth shape having 8 white (transparent) and 8 black (opaque) spokes. Because the carrier frequency is varied according to target positions, its modulation signal is similar to the frequency modulation (FM). The displacement and phase of its frequency contain an azimuth of targets. The con-scan reticle generates a stable circular trace as a target locates at an optical axis.

The signal processing of the con-scan reticle seeker is shown in Fig. 7. The output signal of the detector passes the automatic gain controller (AGC), and then its carrier signal is extracted by the carrier BPF. The amplitude of the carrier signal is limited by a limiter. The frequency discriminator detects higher frequency components of the carrier signal, and then it is increased by an envelope detector. So it results in an AM. The spinning frequency components are

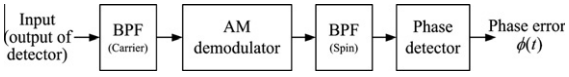

Fig. 5. Signal processing procedure of spin-scan seeker.

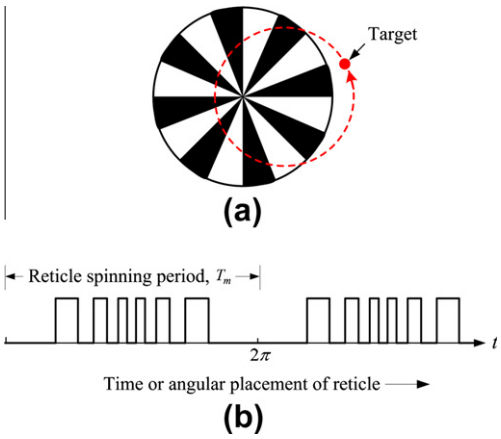

Fig. 6. (a) Structure and (b) its output pulse of con-scan reticle seeker.

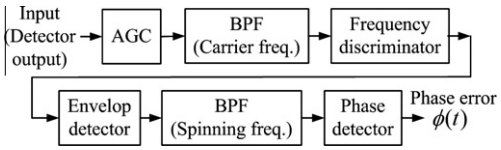

Fig. 7. Signal processing procedure of con-scan reticle seeker.

extracted by the second BPF in Fig. 7, because the output signal of the envelope detector has a period due to the nutation spinning. Phase detector estimates the azimuth angle of targets by comparing with the standard phase of the nutation spinning.

4. Directed infrared countermeasures (DIRCM) jamming

4.1. DIRCM jamming of spin-scan reticle seeker

Fig. 8 shows the outline for modulated jamming to spin-scan reticle seeker. It considers a general case of a target with a collocated jammer that is modulated in time. The radiation power seen at the detector, $P_d(t)$ is represented by

$$P_d(t) = [A + P_j(t)]m_r(t) \tag{2}$$

where A is the target radiation power falling on the reticle and $P_j(t)$ is the time-modulated jammer power arriving at the reticle [7]. And $m_r(t)$ is the reticle modulation function as shown in Fig. 9a and it can be expressed by

$$m_r(t) = \frac{1}{2}[1 + \alpha m_t(t)\sin\omega_c t] \tag{3}$$

where α $(0 \leqslant \alpha \leqslant 1)$ is a constant representing the modulation efficiency and $m_t(t)$ is a carrier gating function as shown in Fig. 9b and ω_c is a carrier angular frequency. $m_t(t)$ is a square wave with a reticle angular frequency (spinning frequency), ω_m and a duty fac-

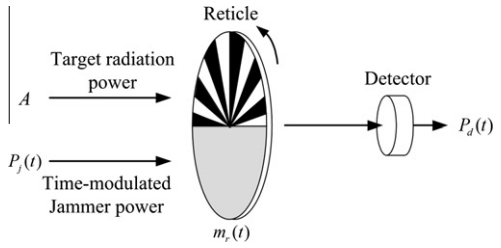

Fig. 8. Outline for modulated jamming to spin-scan reticle seeker.

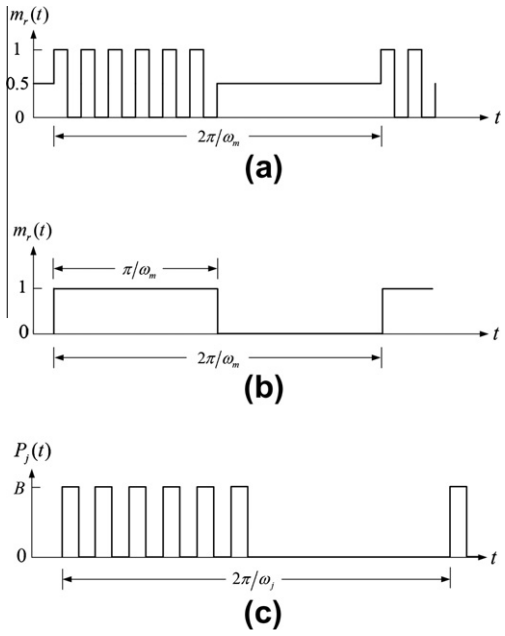

Fig. 9. Waveforms of (a) spin-scan reticle modulation function, (b) carrier modulation function and (c) jammer modulation.

tor of 50%. Assume that the jammer modulation, $P_j(t)$ also has a carrier form at the frequency, ω_{cj} and is gated at the jammer frequency, ω_j as shown in Fig. 8c and it can be expressed by

$$P_j(t) = \frac{B}{2} m_j(t)(1 + \sin \omega_{cj} t) \tag{4}$$

where $m_j(t)$ has the same form as $m_t(t)$, except that ω_m is replaced by ω_j. And B is the peak of the jammer power.

Assume that jammer carrier frequency, ω_{cj} is same as the carrier frequency of the seeker, ω_c. By using Eqs. (3) and (4), Eq. (2) is converted to

$$P_d(t) = \frac{1}{2}\left[A + \frac{1}{2} B m_j(t)(1 + \sin \omega_c t)\right] \cdot [1 + \alpha m_t(t) \sin \omega_c t] \tag{5}$$

Assuming that the carrier amplifier passes only signals near the carrier frequency, the output of the carrier amplifier can be approximated by

$$S_c(t) \approx \alpha \left[A + \frac{1}{2} B m_j(t)\right] m_t(t) \sin \omega_c t + \frac{1}{2} B m_j(t) \sin \omega_c t \tag{6}$$

The envelope of the carrier modulation, $S_e(t)$ in Eq. (6) given by

$$S_e(t) \approx \alpha A m_j(t) + \frac{B}{2} m_j(t)[1 + \alpha m_t(t)] \tag{7}$$

The envelope signal, $S_e(t)$ is further processed by a precession amplifier, which is tuned around the spinning frequency, ω_m.

Assuming that ω_j is close to ω_m, the seeker driving signal, $P(t)$ is given by

$$P(t) \approx \alpha \left(A + \frac{B}{4}\right) \sin \omega_m t + \frac{B}{2}\left(1 + \frac{\alpha}{2}\right) \sin[\omega_j t + \phi_j(t)] \tag{8}$$

where $\phi_t(t)$ is a jammer phase difference of ω_j and ω_m.

The azimuth angle of the target is related to the phase difference between $P(t)$ and the ω_m. Through a low-pass filter (LPF) after product of $P(t)$ and $\exp(j\omega_m t)$, the azimuth phase difference, $\phi(t)$ can be derived by

$$\phi(t) \approx \alpha \left(A + \frac{B}{4}\right) + \frac{B}{2}\left(1 + \frac{\alpha}{2}\right) \exp[j\beta(t)] \tag{9}$$

where $\beta(t) = (\omega_m - \omega_j)t - \phi_j(t)$. $\phi(t)$ actuates a spinning gyro (rotating magnet). If jammer signal does not exist ($B = 0$), an image point (target point) moves toward the center of the reticle along the in-phase direction with a rate proportional to αA, where it reaches the equilibrium state. On the other hand, if jammer signal exists ($B \neq 0$), it results in the disturbance for the missile tracking.

4.2. DIRCM jamming of con-scan reticle seeker

The jamming process of con-scan reticle seeker is similar to that of spin-scan reticle seeker. Fig. 10 shows output signals of a detector in the con-scan reticle seeker. A jammer signal $j(t)$ with a peak jammer power B and a period T_j is shown in Fig. 10a. In case the target radiation power A and the jammer signal $j(t)$ is simultaneously arrived to the con-scan reticle, the sum of the two signals $s(t)$ is shown in Fig. 10b. Fig. 10c represents the reticle modulation function, where T_r means the staying time of a target on the reticle. Fig. 10d represents an effective signal $S_e(t)$ inputted to the detector through the con-scan reticle. Through the signal processing procedure of Fig. 7 in Section 3.2, the effective signal produces a phase detector output (phase error signal) $\varphi(t)$. $\varphi(t)$ is given by

$$\phi(t) \approx C \cdot \exp[-j(\Delta\omega t - \pi\rho_j)] + D \tag{10}$$

where $\Delta\omega = \omega_j - \omega_m$ and ρ_j is the duty ratio of the jammer pulse. C and D are constants related to the reticle modulation factor and the jammer modulation factor.

5. Reticle seeker simulator and jamming effect analysis

In order to analyze the jamming effect of the spin-scan and con-scan seeker, we implemented a reticle seeker simulator using the MATLAB SIMULINK 7.4 version. Since SIMULINK offers various functions and can make user definition function linked with MAT-

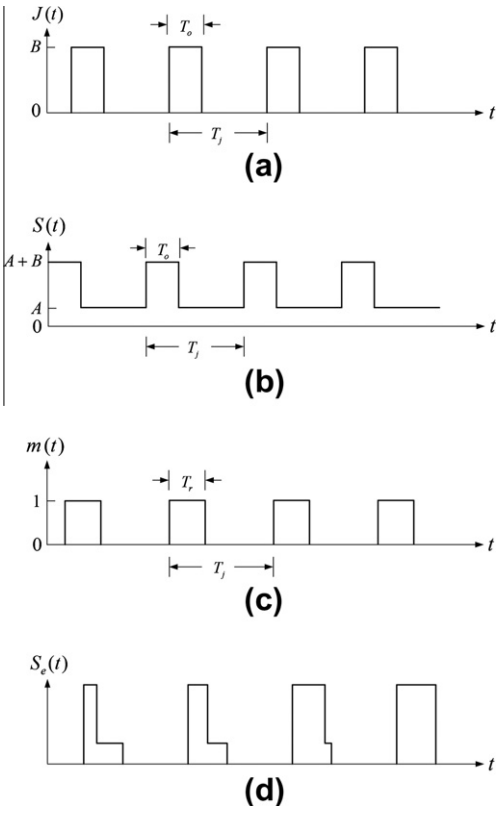

Fig. 10. Output signals of detector included jammer signal. Waveforms of (a) jammer signal, (b) combined target and jammer, (c) reticle modulation function, and (d) effective signal inputted to the detector.

LAB, it can perform various computer simulations. In this paper, it assumed that one circular target is moving on the reticle. And experiments were performed by relative magnitude of target signal and jammer signal, instead of the radiation power of an IR source. The simulator contains a jammer block producing a jammer signal and the jammer signal is generated by variable frequency.

5.1. Spin-scan seeker simulator

Fig. 11 shows the block diagram for signal processing of spin-scan reticle used in simulations. In case a target of arbitrary position passes through the reticle block, it can obtain a reticle modulation signal according to a target position. The reticle modulation block generates its signal using the rotational reticle image set to radius of 0.5 with 240 × 240 size. *x* and y represent the target position from a missile viewpoint. The jammer block controlling frequency and power of a jammer signal generates the jammer signal, inputted to the spin-scan reticle. We set the carrier frequency, f_c = 1.2 kHz, the spinning frequency, f_m = 100 Hz, the sampling frequency, f_s = 36 kHz. The reticle modulation signal and the jammer signal are inputted to the first BPF with the intermediate frequency of 1.2 kHz and the bandwidth of 500 Hz, to extract a carrier frequency. At this time, the used BPF is the second-order Butterworth filter. The carrier frequency, passing through the first BPF, is entered to an AM demodulator in order to detect the amplitude of the carrier pulse. The amplitude of the spin-scan reticle modulation signal of Fig. 9a is decreased, as the target moves to the center of the reticle; the amplitude, on the other hand, is increased, as the target is away from the center of the reticle. So this is similar to the AM modulation. So, the AM demodulator can estimate the radial coordinates of the target. And then, the output signal of the AM demodulator entered the second BPF with the intermediate frequency of 100 Hz and the band width of 20 Hz. The output signal of the second BPF enters the phase detector to estimate the azimuth angle of the target. In order to obtain the azimuth angle of the target, a standard sine wave is used. In Fig. 11 and 14, a tracking block is simply approximated to a low-pass filter (LPF) for reducing of tracking error. As shown in these figures, a missile tracks the *x* and *y* position of the target according to the tracking loop.

Fig. 12 shows the output waveforms of the spin-scan reticle, as the spinning reticle rotates. It assumed that the target position exists at (0.2, 0.2) on the reticle. Fig. 12a and b show the respective reticle output signals for non-jamming and jamming. The output of the reticle is 1 at white (transparent) spokes and 0 on black (opaque) spokes. We set the target energy magnitude as 1, the jammer signal magnitude as 3, jammer frequency as 90 Hz.

Fig. 13a and b show the tracking results of the target during 10 rotations of the reticle for non-jamming. Fig. 13a shows a tracking result for the target position of (0.2, 0.2). As shown in the figure, as a target positions (*x* and *y* values) is close to zero, a missile tracks the target. Likewise, Fig. 13b shows a tracking result of the target position of (−0.3, −0.1). As shown in the figure, we can know that the missile can track the target, as the target moves to the reticle's center. Fig. 13c and d show a tracking result for jamming (in case the target signal and the jammer signal are together inputted to the reticle). In order to analyze effects of the jammer signal, it assumed that a target comes to a stand on the reticle. The figures show the tracking result during 300 ms, 30 rotations of the reticle. Fig. 13c shows a tracking result for jamming after 100 ms, in case a target exists on (0.2, 0.2) of the reticle. At this time, the frequency of the jammer signal is set to 90 Hz. As shown in figures, in case of non-jamming, the missile tracks the target well, as the target is close to the reticle's center. But, after 100 ms, we can show that the missile fails to track the target because the missile mistakes the target for being away from the reticle's center and rotating on the reticle by the jammer signal. Fig. 13d shows a tracking result for jamming after 100 ms, in case the target exists on (−0.3, −0.1) of the reticle. We can know that the missile can not track the exact target position.

5.2. Con-scan seeker simulator

Fig. 14 shows a block diagram for signal processing of con-scan reticle used in simulations. We set the spinning frequency f_m = 100 Hz, the sampling frequency f_s = 36 kHz. Like the spin-scan reticle seeker, its input signal is made by reticle modulation signal and jammer signal for a target of arbitrary position. And then, if the input signal passes through the first BPF with the intermediate frequency of 1.6 kHz and the band width of 500 Hz, its carrier frequency component is obtained. The amplitude modulation signal is acquired using a frequency discriminator implemented by high-pass filter (HPF). As the amplitude modulation signal passing through the envelope detector (AM demodulator) is inputted to the second BPF with the intermediate frequency of 100 Hz and the band width of 20 Hz, the target position can be extracted. The con-scan reticle block generates the reticle modulation signal using the con-scan reticle image with 240 × 240 pixel size. And it assumed that the rotation radius on the reticle of target is 60% of the reticle radius. And we set the radius of the reticle image as 0.5 [17].

Fig. 15 shows the output waveforms of the con-scan reticle for analysis of jamming effect. The con-scan reticle is fixed and the figures show the reticle's output waveforms of a target through its

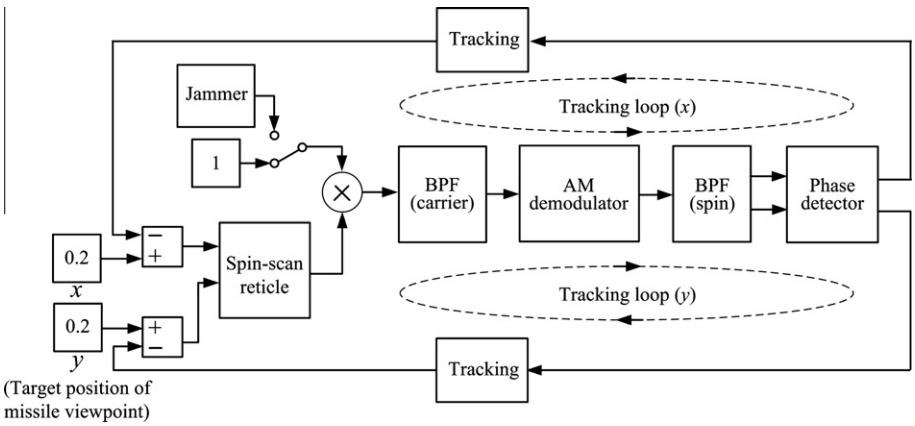

Fig. 11. Block diagram for signal processing of spin-scan reticle used in simulations.

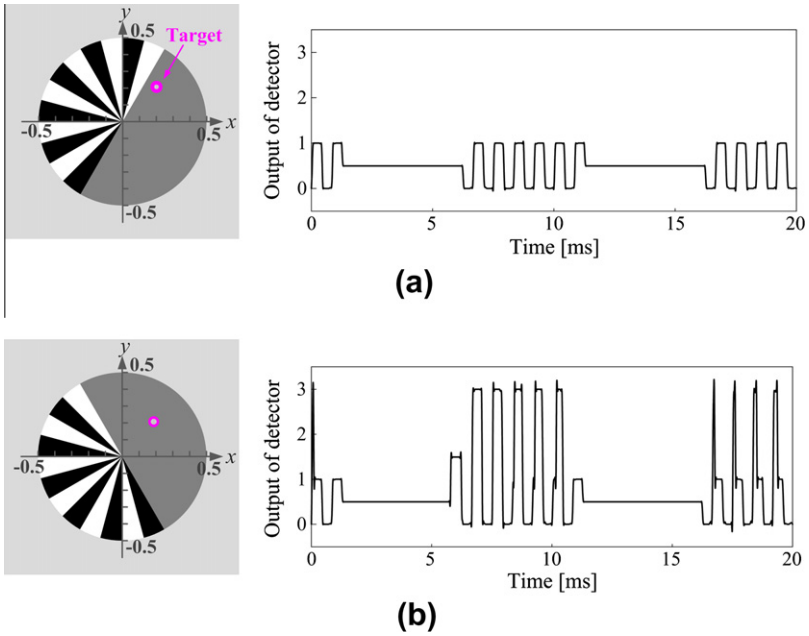

Fig. 12. Output waveforms of spin-scan reticle for (a) non-jamming and (b) jamming.

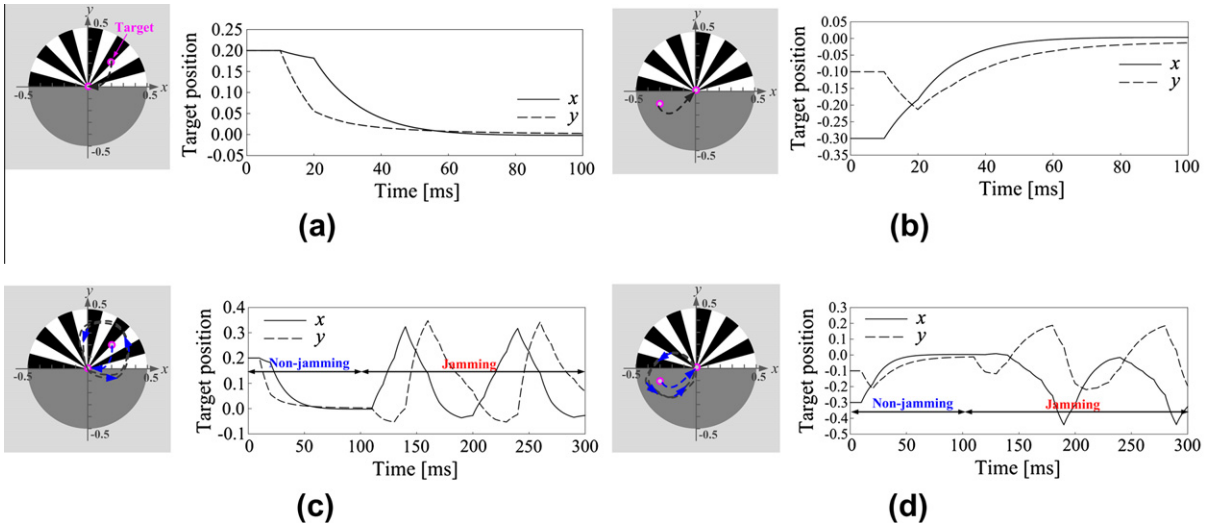

Fig. 13. Tracking results of spin-scan reticle for target position of (a) (0.2, 0.2) and (b) (−0.3, −0.1) for non-jamming, (c) (0.2, 0.2) and (d) (−0.3, −0.1) for jamming after 100 ms.

optical rotation. The target exists at (0.2, 0.2) on the reticle. Fig. 15a and b show the respective reticle output signals for non-jamming and jamming. The frequency of the jammer signal is set to 90 Hz.

Fig. 16a and b show the tracking results of the con-scan reticle at respective target positions for non-jamming. Fig. 16a shows a tracking result at the target position of (0.2, −0.3). As shown in figure, as target position (x and y values) are close to zero, target can be tracked exactly. Likewise, Fig. 16b shows a tracking result at the target position of (−0.2, 0.2). In the figures, we can know that a missile tracks the target, as the target moves to the reticle's center. Fig. 16c and d show the tracking results for jamming during 300 ms. Like the spin-scan reticle's simulation, it assumes that a target comes to a stand on the reticle. Fig. 16c shows the tracking result for jamming after 100 ms, in case a target exists at (0.2, −0.3) on the reticle. At this time, the frequency of the jammer signal is set to 90 Hz. As shown in the figures, the target is exactly tracked, as the target moves to the reticle's center at non-jamming. The target, on the other hand, recedes from the reticle's center at jamming after 100 ms and escape from the reticle after 200 ms. In Fig. 16d, we can show that the missile mistakes the target for rotating on the reticle, in case the target exists at (−0.2, 0.2) on the reticle.

5.3. Jamming effect analysis of reticle seeker

In order to analyze the jamming effect of the two reticle seekers, the spin-scan and con-scan reticle seeker, tracking performance of reticles is simulated according to frequencies of the jammer signal. The frequency range of the jammer signal is from 50 Hz to 130 Hz and its magnitude was equally set according to jammer frequencies.

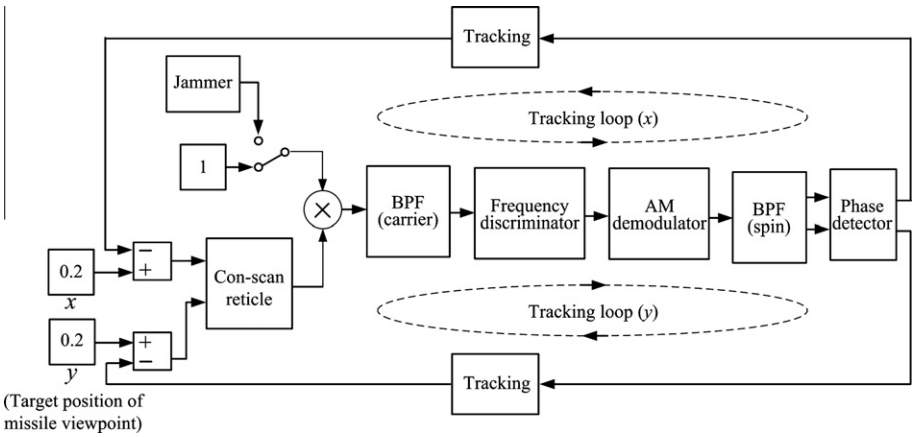

Fig. 14. Block diagram for signal processing of con-scan reticle used in simulation.

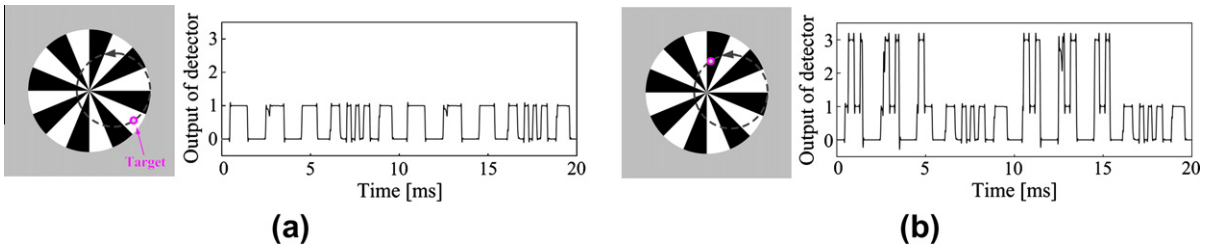

Fig. 15. Output waveforms of con-scan reticle for (a) non-jamming and (b) jamming.

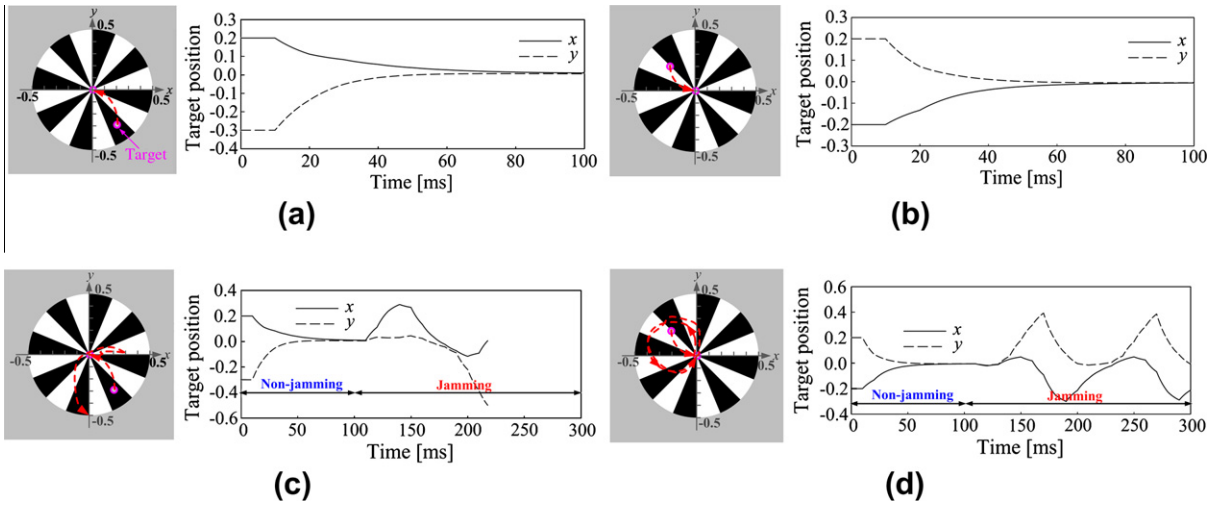

Fig. 16. Tracking results of con-scan reticle for target position of (a) (0.2, −0.3) and (b) (−0.2, 0.2) for non-jamming, (c) (0.2, −0.3) and (d) (−0.2, 0.2) for jamming after 100 ms.

Fig. 17 shows tracking results for various jammer frequencies in the spin-scan reticle. Until 100 ms, during the spin-scan reticle rotates 10 times, only target signal is inputted to the reticle (Non-jamming). After 100 ms, the target signal and jammer signal are together inputted to reticle (Jamming). In Fig. 17a, in case of the jammer frequency of 80 Hz, we can know that a target deviates slightly from the reticle's center but the jamming effect is not remarkable. Fig. 17b shows a tracking result for the jammer frequency of 95 Hz. Because the target deviates from the reticle's center and rotates on the reticle due to variation of x, y error values, it is difficult to detect the target. In Fig. 17c, in case of the jammer frequency of 95 Hz, we can show that the target deviates from the reticle and the target tracking is failed due to the jammer signal after 160 ms. In Fig. 17d, in case of the jammer frequency of 100 Hz, we can show that the jamming effect decreases noticeably, in case the phase of the jammer frequency is equal to that of the spin-scan reticle frequency. This means that the target signal and the jammer signal are overlapped and, hence it is easy to detect the target. Therefore we can confirm that the jamming effect is superior, in case the jammer frequency is 100 Hz and its phase difference is non-zero.

In the simulation of the spin-scan reticle, we use $\bar{\phi}(t)$, the average value of the phase detector output per the reticle's spinning as a phase error by

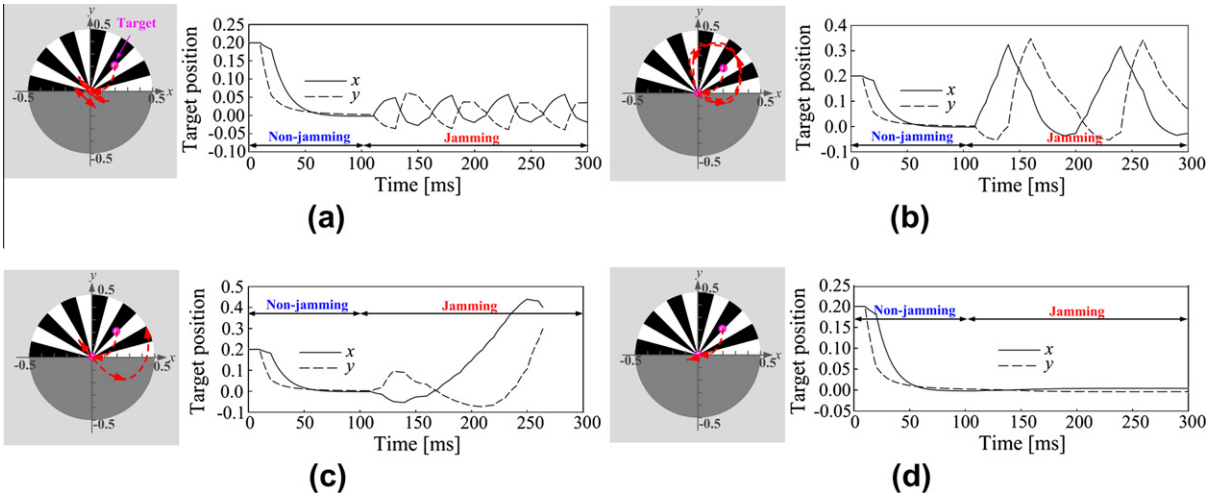

Fig. 17. Tracking results of spin-scan reticle according to jammer frequency. (a) 80 Hz, (b) 90 Hz, (c) 95 Hz and (d) 100 Hz.

$$\bar{\phi}(t) = \frac{1}{T_m}\int_0^{T_m} \phi(t)\, dt \tag{11}$$

where T_m is the spinning period of the reticle, $T_m = 2\pi/\omega_m$. Fig. 18 shows the variance of the average phase error $\bar{\phi}(t)$, in case the range of the jammer frequency f_j is from 10 Hz to 1 kHz in the spin-scan reticle. B means the relative IR jammer intensity. In the figure, we can know that the jamming effect is significantly increased in case jammer frequency and reticle frequency are similar. Fig. 19 shows the average phase error $\bar{\phi}$ for $f_j = 95$ Hz. In case of $B = 0$, $\bar{\phi}$ is converged 0.05 as jammer frequency increase and the variance of it has 0. However the presence of jammer signal results in sinusoidal perturbation of $\bar{\phi}$, which induce missile to miss track.

Fig. 20 shows a 3D trajectory of a missile with the spin-scan reticle under non-jamming and jamming. And Table 1 shows an engagement scenario, including the initial position, the velocity of a target and a missile. The missile is jammed after 1 s from the initial position and is guided by PNG. We set that the jammer frequency, $f_j = 102$ Hz and the spinning frequency, $f_m = 100$ Hz. The missile is jammed for 1 s, then it nutates around the target in large circular motion with two raps. Since the frequency difference between the jammer modulation and reticle spinning is 2 Hz, the seeker LOS and missile motion are rotated during two turns as shown in Eq. (9).

Fig. 21 shows tracking results for various jammer frequencies in the con-scan reticle. The tracking result is similar to the case of the spin-scan reticle. Fig. 21a shows that the target is close to the ret-

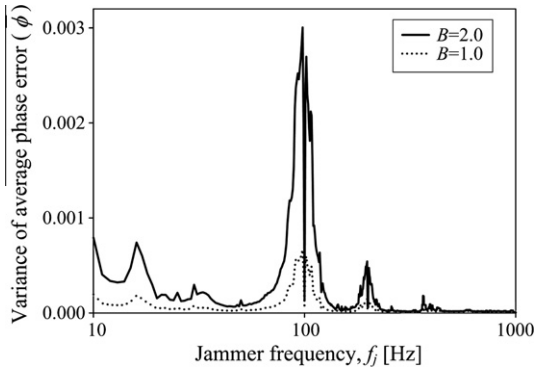

Fig. 18. Variance of average phase error $\bar{\phi}$ for jammer frequency f_j in spin-scan reticle.

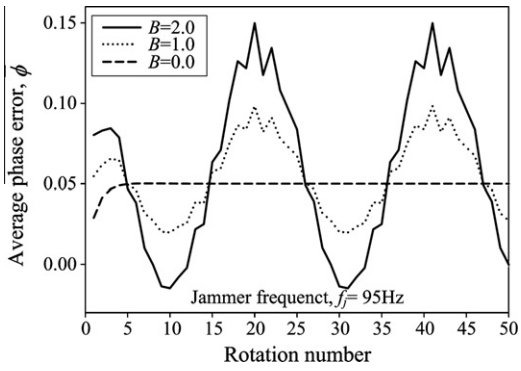

Fig. 19. Average phase error $\bar{\phi}$ for $f_j = 95$ Hz in spin-scan reticle.

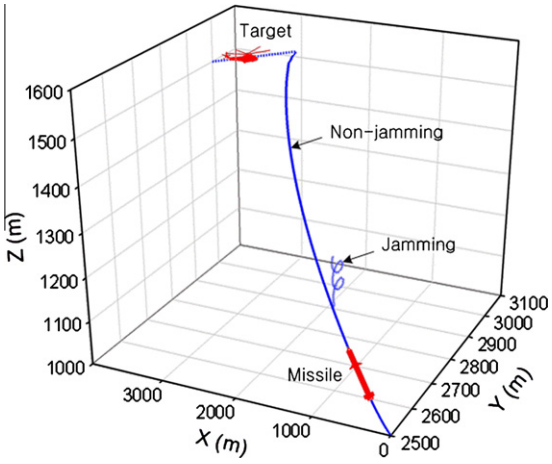

Fig. 20. 3D trajectory of missile under non-jamming and jamming.

Table 1
Engagement scenario.

	Initial position (m)	Velocity (m/s)	Navigation
Target	$X = 4000$, $Y = 3000$, $Z = 1500$	250	–
Missile	$X = 0$, $Y = 2500$, $Z = 1000$	600	PNG

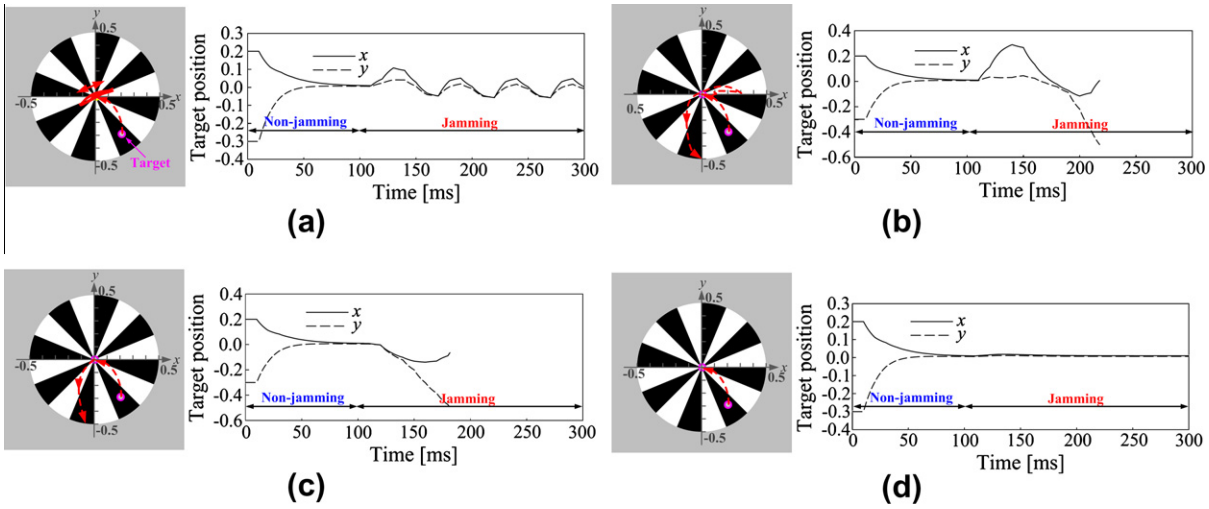

Fig. 21. Tracking results of con-scan reticle according to jammer frequency. (a) 80 Hz, (b) 90 Hz, (c) 95 Hz and (d) 100 Hz.

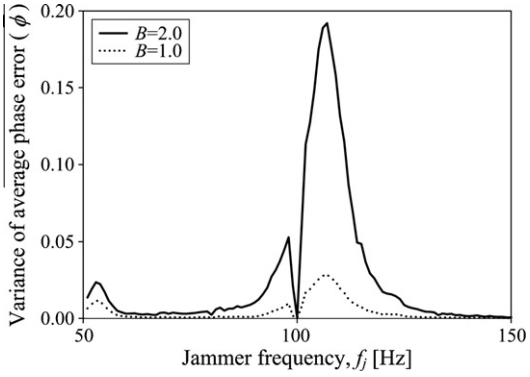

Fig. 22. Variance of average phase error $\bar{\phi}$ for the jammer frequency f_j in con-scan reticle.

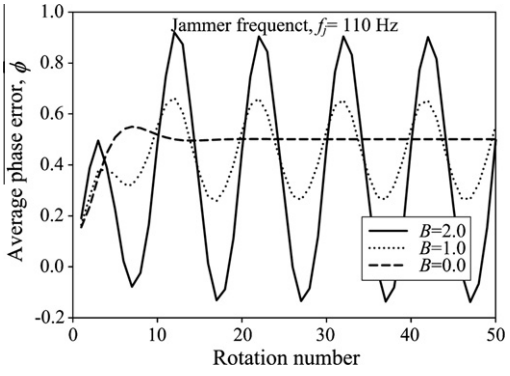

Fig. 23. Average phase error $\bar{\phi}$ for $f_j = 110$ Hz in con-scan reticle.

icle's center for the jammer frequency of 80 Hz. But, in Fig. 21b and c, we can show that the target deviates from the reticle's center and tracking target is failed. In case of the jammer frequency of 90 Hz, the target deviation time from the reticle is after about 220 ms. In case of the jammer frequency of 90 Hz, the deviation time is after about 180 ms. In here, we can know that the more the jammer frequency is close to 100 Hz, the more the jamming effect is superior. In Fig. 21d, we can show that a target can be tracked regardless of effect of the jammer signal, in case the jammer frequency is 100 Hz and the phase of the spinning frequency and the jammer frequency is same.

Fig. 22 shows the variance of the average phase error $\bar{\phi}(t)$, in case the range of the jammer frequency f_j is from 50 Hz to 150 Hz in the con-scan reticle. Like the case of the spin-scan reticle, we can know that the jamming effect is significantly increased in case jammer frequency and reticle frequency are similar. Fig. 23 shows the average phase error $\bar{\phi}$ for $f_j = 110$ Hz. In case of $B = 0$, $\bar{\phi}$ is converged 0.5 as jammer frequency increase and the variance of it has 0. However, Like the case of the spin-scan reticle, the presence of jammer signal introduces sinusoidal perturbation of $\bar{\phi}$, which induce missile to miss track. Notice that the sinusoidal wave number of phase error $\bar{\phi}$ is five in 0.5 s (10 Hz).

The simulation results of the con-scan jamming effect are similar to that of the spin-scan. As shown in Eq. (10), since the average phase error $\bar{\phi}$ is related with the difference frequency, $\Delta\omega = \omega_j - \omega_m$, the missile motion under jamming nutates around the target in the large circle with the difference frequency.

To confirm the jamming effect quantitatively, we used the correlation coefficient given by

$$\rho_{XX_j} = corr(X, X_j) = \frac{E[(X - \mu_X)(X_j - \mu_{X_j})]}{\sigma_X \sigma_{X_j}} \tag{12}$$

where X and X_j are the target position of the missile viewpoint at non-jamming (in case the missile can track the target well) and jamming (in case the missile can not track the target well). If the jamming is not completely effective, this correlation coefficient becomes one ($\rho_{XX_j} = 1$). But, if the jamming is effective, the range is $0 < \rho_{XX_j} < 1$. If the correlation coefficient is less than one and close

Table 2
Correlation coefficient for various jammer frequencies in spin-scan and con-scan reticle seeker.

Jammer frequency (Hz)	Correlation coefficient for jamming	
	Spin-scan seeker	Con-scan seeker
50	0.99	0.99
60	0.99	0.99
70	0.97	0.95
80	0.92	0.89
90	0.27	0.12
95	0.15	0.09
100	0.98	0.97
105	0.29	0.24
110	0.42	0.30
120	0.96	0.88
130	0.98	0.99

to zero, this means that the missile can not track well due to high jamming effect. Table 2 shows the correlation coefficients for various jammer frequencies in the spin-scan and con-scan reticle seeker. As shown in Table 2, we can confirm that the jamming effect is superior in the vicinity of 100 Hz, being similar to the spinning frequency. In case the jammer frequency and the spinning frequency have same phase at 100 Hz, we can show that the jamming effect is very low. The jamming effect, on the other hand, will be much larger if the two frequencies have not same phase.

6. Conclusions

In this paper, we implemented the reticle seeker simulator on MATLAB-SIMULINK in order to analyze jamming effect in the directed jammer methods. And we evaluated jamming effect by using correlation coefficients for jamming, as an evaluation criterion of jamming performance. This simulator can be also used to analyze flare countermeasure effect as well as jamming effect for various kinds of reticles. And blocks containing various variables, which can be considered under real circumstances, can be added to this simulator. The experimental results show that jamming effect is greatly influenced by frequency, phase and intensity of jammer signal. Specially, jammer frequency has the largest influence on the jamming effect. Our simulation results show that jamming effect is significantly increased when jammer frequency is similar to spinning frequency. In viewpoints of scientific research, we implemented this jamming effect simulator facilitates jamming effect analysis as well as understanding of signal processing for two reticle seekers. In this simulator, a jammer needs to know frequency characteristics of a jammed missile seeker for maximum jamming effect, before an effective DIRCM jammer signal is added to the missile signal. So, an important future work for this simulator is about automatic detection of jammer frequency for a jammed missile seeker. Since then, this simulator with automatic jammer frequency detector can be applied to real-time missile circumstance.

Acknowledgment

This work was supported by a basic research project of ADD (Agency for defense development) in Korea.

References

[1] T.W. Bae, Y.C. Kim, S.H. Ahn, K.I. Sohng, An efficient two-dimensional least mean square (TDLMS) based on block statistics for small target detection, Journal of Infrared, Millimeter and Terahertz Waves 30 (10) (2009) 1092–1101.
[2] T.W. Bae, Y.C. Kim, S.H. Ahn, K.I. Sohng, A novel two-dimensional LMS (TDLMS) using sub-sampling mask and step-size index for small target detection, IEICE Electronics Express 30 (10) (2010) 112–117.
[3] T.W. Bae, F. Zhang, I.S. Kweon, Edge directional 2D LMS filter for infrared small target detection, Infrared Physics & Technology 55 (1) (2012) 137–145.
[4] T.W. Bae, K.I. Sohng, Small target detection using bilateral filter based on edge component, International Journal of Infrared Millimeter Terahertz Waves 31 (6) (2010) 735–743.
[5] T.W. Bae, Y.C. Kim, S.H. Ahn, K.I. Sohng, Small target detection using the bilateral filter based on target similarity index, IEICE Electronics Express 7 (9) (2010) 589–595.
[6] X. Bai, F. Zhou, Y. Xie, New class of top-hat transformation to enhance infrared small targets, Journal of Electronic Imaging 17 (3) (2008) 0305011-1–0305013-1.
[7] T.W. Bae, B.I. Kim, F. Zhang, Y.C. Kim, S.H. Ahn, K.I. Sohng, Recursive multi-SEs NWTH method for small target detection in infrared images, IEICE Electronics Express 8 (19) (2011) 1576–1582.
[8] F. Zhang, C. Li, L. Shi, Detecting and tracking dim moving point target in IR image sequence, Infrared Physics & Technology 46 (2005) 323–328.
[9] T.W. Bae, B.I. Kim, Y.C. Kim, K.I. Sohng, Small target detection using cross product based on temporal profile in infrared image sequences, Computers & Electrical Engineering 36 (6) (2010) 1156–1164.
[10] T.W. Bae, Small target detection using bilateral filter and temporal cross product in infrared images, Infrared Physics & Technology 54 (5) (2011) 403–411.
[11] D.H. Titterton, A review of the development of optical countermeasures, Proceedings of SPIE 5615 (2004) 1–15.
[12] D. Winterfeldt, T. O'Sullivan, Should we protect commercial airplanes against surface-to-air missile attacks by terrorists?, Decision Analysis 3 (2) (2006) 63–75
[13] J. Heikell, Electronic warfare self-protection of battlefield helicopters: a holistic view, Applied Electronics Laboratory Series E: Electronics Publications E18, Helsinki University of Technology, Espoo, 2005.
[14] D.H. Pollock, Countermeasure systems, in: The Infrared & Electro-Optical Systems Handbook 7, SPIE Optical Engineering Press, Bellingham, WA, 1993, pp. 235–286.
[15] D.W. Fisher, R.F. Leftwich, H.W. Yates, Survey of infrared trackers, Applied Optics 5 (4) (2007) 507–515.
[16] R.G. Driggers, C.E. Halford, G.D. Boreman, Parameters of spinning AM reticles, Applied Optics 30 (19) (1991) 2675–2684.
[17] H.K. Hong, S.H. Han, J.S. Choi, Simulation of the spinning concentric annular ring reticle seeker and an efficient counter-countermeasure, Optical Engineering 36 (11) (1997) 3206–3211.
[18] G. Olsson, Simulation of reticle seekers by means of an image processing system, Optical Engineering 33 (3) (2009) 730–736.
[19] http://www.ontar.com/Software/.
[20] E. Koch, Review on pyrotechnic aerial infrared decoys, in: International Peer-Reviewed Journal on Energetic Materials Official Journal of the International Pyrotechnics Society, vol. 260, 2001, pp. 3–11.
[21] S.H. Han, H.K. Hong, J.S. Choi, Dynamic simulation of infrared reticle seekers and an efficient counter-countermeasures algorithm, Optical Engineering 36 (8) (1997) 2341–2345.
[22] C.K. Kovach, J.S. Gauthier, A missile system simulation benchmark using the ACSL graphic modeler, American Institute of Aeronautics and Astronautics (2001) 1–9.
[23] P. Zarchan, Tactical and Strategic Missile Guidance, second ed., American Institute of Aeronautics and Astronautics, Washington-United States, 1994.
[24] S.H. Ahn, Y.C. Kim, T.W. Bae, B.I. Kim, K.H. Kim, DIRCM jamming effect analysis of spin-scan reticle seeker, in: Proceedings of the 2009 IEEE 9th Malaysia International Conference on Communications, 2009, pp. 15–17.
[25] G.Y. Kim, B.I. Kim, T.W. Bae, Y.C. Kim, S.H. Ahn, K.I. Sohng, Implementation of a reticle seeker missile simulator for jamming effect analysis, in: Proceedings of the 2010 IEEE Second International Conference on Image processing Theory, Tools and Applications, 2010.

Update

Infrared Physics and Technology
Volume 56, Issue , January 2013, Page 100

DOI: https://doi.org/10.1016/j.infrared.2012.12.013

Infrared Physics & Technology 56 (2013) 100

Contents lists available at SciVerse ScienceDirect

Infrared Physics & Technology

journal homepage: www.elsevier.com/locate/infrared

Corrigendum

Corrigendum to "Jamming effect analysis of infrared reticle seeker for directed infrared countermeasures" [Infrared Phys. Technol. 55/5 (2012) 431–441]

Tae-Wuk Bae [a], Byoung-Ik Kim [b], Young-Choon Kim [c], Sang-Ho Ahn [d,*]

[a] Stanford Center for Image Systems Engineering, Stanford University, CA 94305, USA
[b] School of Electrical Engineering and Computer Science, Kyungpook National University, South Korea
[c] Dept. of Information and Communication Engineering, Youngdong University, South Korea
[d] Dept. of Electronic Engineering, Inje University, South Korea

The authors regret that there has been a change in the corresponding author of the paper titled "Jamming effect analysis of infrared reticle seeker for directed infrared countermeasures" published in issue "55/5". Dr. Sang Ho Ahn (4th author of the published paper) will be the new corresponding author.

The authors regret the inconvenience caused.

DOI of original article: http://dx.doi.org/10.1016/j.infrared.2012.05.001
* Corresponding author.
E-mail address: nanninggo@gmail.com (S.-H. Ahn).

http://dx.doi.org/10.1016/j.infrared.2012.12.013